Role of Citric Acid in the Formation of Silver Nanoplates through a Synergistic Reduction Approach

ARTICLE *in* LANGMUIR · DECEMBER 2009

Impact Factor: 4.46 · DOI: 10.1021/la903470f · Source: PubMed

4 AUTHORS, INCLUDING:

Xuchuan Jiang
Monash University (Australia)
104 PUBLICATIONS **4,469** CITATIONS
SEE PROFILE

Aibing Yu
University of New South Wales
621 PUBLICATIONS **11,678** CITATIONS
SEE PROFILE

Langmuir
Article
pubs.acs.org/Langmuir

Role of Citric Acid in the Formation of Silver Nanoplates through a Synergistic Reduction Approach

X. C. Jiang,*[,†] C. Y. Chen,[†,‡] W. M. Chen,[†] and A. B. Yu[†]

[†]*School of Materials Science and Engineering, University of New South Wales (UNSW), Sydney, New South Wales 2052, Australia and* [‡]*Key Laboratory for Anisotropy and Texture of Materials (Ministry of Education), School of Materials and Metallurgy, Northeastern University, Shenyang 110004, China*

Received September 14, 2009. Revised Manuscript Received November 13, 2009

This study discusses the function of citrate ions in the synthesis of silver nanoplates through a synergetic reduction approach in ambient conditions. It was found that the citrate ions can play multiple roles in the synthesis process, including a reducing agent, a stabilizer, and a complex agent, and they show some unique features under the reported conditions. The reducing ability of these citrate ions was shown to be weaker than that of sodium borohydride and/or L-ascorbic acid used in the same system. The stability in the shape/size control of silver particles is weaker than that of other surfactants tested in the present system, such as bis(2-ethylhexyl)sulfosuccinate (AOT) and thiols. Citrate ions could form a silver complex with silver ions as $[Ag_2^+\cdots\text{citrate}]$ or $[Ag_3(C_6H_5O_7)_{n+1}]^{3n-}$, as confirmed by electrospray ionization (ESI) mass spectrometry and the kinetic analysis that the molar ratio of citric acid or sodium citrate to silver ions can greatly influence the reaction rate and, hence, the particle growth of silver nanoparticles. Such a complexing effect is further confirmed by the use of chelating ions (e.g., $[Fe(CN)_6]^{4-}$) to form $Ag_n[Fe(CN)_6]^{n-4}$, which can largely influence the synthesis of silver nanoparticles. These results show some formation results of generating silver nanoplates involving citrate ions, which are useful in the shape-controlled synthesis of other metallic nanoparticles with desirable functionalities.

1. Introduction

Because of their fascinating physicochemical properties, metal nanoparticles have attracted intensive research interests such as optical, electronic, magnetic, and chemical.[1−7] In most cases, control of the shape and size of the nanocrystals is critical and has increasingly attracted attention.[8−27] Among them, low-dimensional metallic silver nanostructures (e.g., rods, wires, plates, disks) have an extreme degree of anisotropy together with corners and edges for generating maximum electromagnetic-field enhancement. These have stimulated not only the development of synthesis, characterization, and mechanistic understanding, but also the exploration of functional applications in many areas, such as near-field optical probes, optical sensors, surface-enhanced Raman spectroscopy, and biomedical labeling.[8−27]

A variety of methods have been reported to control the synthesis of silver nanoparticles with two-dimensional (2D) morphologies for desirable properties, such as the photoinduced method,[28−31] electrochemical method,[32] ultrasonic-assistant

*To whom ccorrespondence should be addressed. E-mail: xcjiang@unsw.edu.au.

(1) El-Sayed, M. A. *Acc. Chem. Res.* **2001**, *34*, 257–264.
(2) Kamat, P. V. *J. Phys. Chem. B* **2002**, *106*, 7729–7744.
(3) Brioude, A.; Jiang, X. C.; Pileni, M. P. *J. Phys. Chem. B* **2005**, *109*, 13138–13142.
(4) Yin, Y.; Alivisatos, P. *Nature* **2005**, *437*, 664–670.
(5) Bohren, C. F.; Huffman, D. R. *Absorption and scattering of light by small particles*; Wiley: New York, 1983.
(6) Bloemer, M. J.; Buncick, M. C.; Warmack, R. J.; Ferrell, T. L. *J. Opt. Soc. Am. B* **1988**, *5*, 2552–2559.
(7) Tao, A.; Kim, F.; Hess, C.; Goldberger, J.; He, R.; Sun, Y.; Xia, Y.; Yang, P. D. *Nano Lett.* **2003**, *3*, 1229–1233.
(8) Shanmukh, S.; Jones, L.; Driskell, J.; Zhao, Y. P.; Dluhy, R.; Tripp, R. A. *Nano Lett.* **2006**, *6*, 2630–2636.
(9) McFarland, A. D.; Young, M. A.; Dieringer, J. A.; Van Duyne, R. P. *J. Phys. Chem. B* **2005**, *109*, 11279–11285.
(10) Muniz-Miranda, M. *Chem. Phys. Lett.* **2001**, *340*, 437–443.
(11) Hashimoto, N.; Hashimoto, T.; Teranishi, T.; Nasu, H.; Kamiya, K. *Sens. Actuators, B* **2006**, *113*, 382–388.
(12) Nicewarner-Peña, S. R.; Freeman, R. G.; Reiss, B. D.; He, L.; Peña, D. J.; Walton Ian, D.; Cromer, R.; Keating, C. D.; Natan, M. J. *Science* **2001**, *294*, 137–141.
(13) Katherine, A.; Willets, K. A.; Van Duyne, R. P. *Annu. Rev. Phys. Chem.* **2007**, *58*, 267–297.
(14) Kelly, K. L.; Coronado, E.; Zhao, L.; Schatz, G. C. *J. Phys. Chem. B* **2003**, *107*, 668–677.
(15) Nie, S.; Emory, S. R. *Science* **1997**, *275*, 1102–1106.
(16) Hache, F.; Ricard, D.; Flytzanis, C. *J. Opt. Soc. Am. B* **1986**, *3*, 1647–1655.
(17) Haglund, R. F., Jr.; Yang, L.; Magruder, R. H., III; Wittig, J. E.; Becker, K.; Zuhr, R. A. *Opt. Lett.* **1993**, *18*, 373–375.
(18) Uchida, K.; Kaneko, S.; Omi, S.; Hata, C.; Tanji, H.; Asahara, Y.; Ikushima, A. J.; Tokizaki, T.; Nakamura, A. *J. Opt. Soc. Am. B* **1994**, *11*, 1236–1243.
(19) Tokizaki, T.; Nakamura, A.; Kaneko, S.; Uchida, K.; Omi, S.; Tanji, H.; Asahara, Y. *Appl. Phys. Lett.* **1994**, *64*, 941–943.
(20) West, R.; Wang, Y.; Goodson, T., III *J. Phys. Chem. B* **2003**, *107*, 3419–3426.
(21) Hamanaka, Y.; Nakamura, A.; Omi, S.; Del Fatti, N.; Vallee, F.; Flytzanis, C. *Appl. Phys. Lett.* **1999**, *75*, 1712–1714.
(22) Okada, N.; Hamanaka, Y.; Nakamura, A.; Pastoriza-Santos, I.; Liz-Marzán, L. M. *J. Phys. Chem. B* **2004**, *108*, 8751–8755.
(23) Pastoriza-Santos, I.; Liz-Marzán, L. M. *J. Mater. Chem.* **2008**, *18*, 1724–1737.
(24) Kowshik, M.; Ashtaputre, S.; Kharrazi, S.; Vogel, W.; Urban, J.; Kulkarni, S. K.; Paknikar, K. M. *Nanotechnology* **2003**, *14*, 95–100.
(25) Mukherjee, P.; Ahmad, A.; Mandal, D.; Senapati, S.; Sainkar, S. R.; Khan, M. I.; Ramani, R.; Parischa, R.; Ajayakumar, P. V.; Alam, M.; Sastry, M.; Kumar, R. *Angew. Chem., Int. Ed.* **2001**, *40*, 3585–3588.
(26) Prasad, B. L. V.; Stoeva, S. I.; Sorensen, C. M.; Klabunde, K. J. *Langmuir* **2002**, *18*, 7515–7520.
(27) Haynes, C. L.; Van Duyne, R. P. *J. Phys. Chem. B* **2001**, *105*, 5599–5611.
(28) Jin, R.; Cao, Y.; Mirkin, C. A.; Kelly, K. L.; Schatz, G. C.; Zheng, J. G. *Science* **2001**, *294*, 1901–1903.
(29) Jin, R.; Cao, Y.; Metraux, G. S.; Schatz, G. C.; Mirkin, C. A. *Nature* **2003**, *425*, 487–490.
(30) Maillard, M.; Huang, P.; Brus, L. *Nano Lett.* **2003**, *3*, 1611–1615.
(31) Callegari, A.; Tonti, D.; Chergui, M. *Nano Lett.* **2003**, *3*, 1565–1568.
(32) Sun, Y. *Chem. Mater.* **2007**, *19*, 5845–5847.
(33) Jiang, L. P.; Xu, S.; Zhu, J. M.; Zhang, J. R.; Zhu, J. J.; Chen, H. Y. *Inorg. Chem.* **2004**, *43*, 5877–5883.
(34) Sun, Y.; Mayers, B.; Xia, Y. *Nano Lett.* **2003**, *3*, 675–679.
(35) Sun, Y.; Xia, Y. *Science* **2002**, *298*, 2176–2179.

method,[33] solvothermal method,[34−38] and templating method (e.g., "soft" reverse micelles and "hard" polystyrene spheres).[39−43] Many experiments have shown that the growth of silver nanocrystals in solution is sensitive to the presence of citric acid or sodium citrate, but the exact role of citrate ions still remains debatable. For instance, Jin et al.[28,29] demonstrated that the citrate ions act as stabilizers in an efficient synthesis method for generating monodispersed silver nanoprisms through illumination of visible light. Henglein and Giersig[44] supposed that citrate ions do not act as reducing agents but solely as stabilizers of the colloidal particles formed in the synthesis of colloidal silver sols using γ irradiation of $AgClO_4$ solutions. Pillai and Kamat[45] demonstrated that citrate ions influence the particle growth at the early stages by complexing with positively charged Ag_2^+ dimers and slow down the cluster growth contributing to the formation of larger silver nanocrystals of varying shape and size. Some investigators described that citrate ions can serve both as reducing agents and as stabilizers.[46−49] Also, Ji et al.[48] suggested that the citrate ions are multifunctional in acting as reducing agents, stabilizers, and pH mediators in the synthesis of gold nanoparticles.

Recently, Kilin et al.[50] demonstrated in the ab initio study that the approximate 3-fold symmetry of citric acid matches that of Ag(111) and results in four Ag−O bonds. In contrast, citric acid forms only two bonds with Ag(100) because of the geometry mismatch. Migration of a hydrogen atom within citric acid activates the electrons of the carboxyl oxygen atom and provides additional binding affinity toward the Ag(111) plane. The preferential binding energy of citric acid to Ag(111) promotes crystal growth along the Ag(100) surface. Mpourmpakis and Vlachos[51] supposed that the citrate ions serve as charge regulators as well as reducing agents and stabilizers through density functional theory simulations. In addition, some studies have shown that the citrate ions can form strong complexes with Ag^+, Fe^{3+}, Ca^{2+}, Mg^{2+}, and Zn^{2+} ions in a solution, which can influence the formation and growth of metal particles.[52,53] However, the nature of citrate ions in the formation of silver nanoplates is still not properly understood, particularly for the system that involves no light illumination and/or γ-ray irradiation. This would impede the progress in the exploitation of functional applications of silver nanoplates. To properly understand the functionalities of citrate ions is still a challenging task in silver nanoparticle research.

In this study, we investigate the role of citrate ions in the shape-controlled synthesis of silver nanoplates through a synergetic reduction method that was recently developed in our work.[54−57] Functions of citrate ions in the formation and growth of silver nanoparticles will then be identified by transmission electron microscopy (TEM) and UV−vis spectrometry techniques. The possible mechanisms in the shape control of silver nanoparticles are finally discussed.

2. Experimental Section

2.1. Chemicals. Silver nitrate ($AgNO_3$, 99.9%), citric acid (99%), sodium citrate (99%), L-ascorbic acid (≥99.0%), sodium borohydride ($NaBH_4$, 99%), sodium bis(2-ethylhexyl)sulfosuccinate (NaAOT, 99%), and potassium ferrocyanide ($K_4[Fe(CN)_6]\cdot 3H_2O$) were all purchased from Sigma-Aldrich and used as received without further treatment. All of the solutions were freshly made for the synthesis of silver nanoparticles, especially the freshly made $NaBH_4$ aqueous solution, which was ice bathed before use. Ultrapure water was used in all of the synthesis processes.

2.2. Synthesis of Silver Nanoplates. The procedure was carried out and modified based on our recent work.[54−57] Briefly, three steps were involved in the procedure as follows. First, 0.625 mL of aqueous $AgNO_3$ (0.02 M) and 1.25 mL of NaAOT (0.02 M) solution were added to a 100 mL conical flask with ultrapure water and then stirred at room temperature for 10 min to ensure a homogeneous solution. The final volume of the mixture was then fixed at 50 mL, and the concentrations of $AgNO_3$ and NaAOT were adjusted at 2.5×10^{-4} and 5.0×10^{-4} M, respectively. Second, 0.15 mL of citrate acid (0.10 M) and 0.125 mL of an L-ascorbic acid (0.10 M) aqueous solution were added to the 50 mL solution and then stirred vigorously to ensure a homogeneous solution. Finally, 0.01 mL of a $NaBH_4$ (0.002 M) aqueous solution was rapidly added into the previously mixed solution and stirred for 30 s. With time, the color of the solution changed from light yellow to purple, then pink, green, and blue. After aging for ∼10 min, the blue solution remained stable at room temperature.

The effects of different experimental parameters were tested by changing the molar ratio of each component to the silver ions accordingly. For example, when increasing the molar ratio of citric acid to silver ions (noted as $[cit]/[Ag^+]$) from 1.2 to 3, 6, 12, 24, and 48, the other parameters (e.g., temperature and concentration of the silver ions, L-ascorbic acid, and sodium borohydride) remained constant. To keep the total volume of the reaction solution, the concentration of the citric acid or sodium citrate stock solution was tuned accordingly.

2.3. Equipment. TEM and selected area electron diffraction (SAED) patterns were conducted under a JEOM 1400 operated at 100 kV. The specimen was prepared by dropping the solution onto the copper grids covered with amorphous carbon and air-dried naturally. The UV−vis absorption spectrum was obtained on a CARY 5G UV−vis spectrophotometer (Varian) with a 1-cm quartz cell. ^{1}H NMR spectra were obtained on a Bruker AVANCE III 500.13 MHz spectrometer at the UNSW NMR Facility. Watergate water suppression was used to reduce the residual water signal. The spectra were obtained in 64 scans with 32 768 data points over a sweep width of 5000 Hz and zero-filled to 65 536 points. Electrospray ionization (ESI) mass spectrometry was carried out by mass spectrometer (model QT of Ultima API, Micromass, Manchester, U.K.) under the conditions of a capillary voltage of 9 kV, a MCP voltage of 2150, and a collision gas of argon.

3. Results and Discussion

3.1. Effect of Citrate Ions. *Citric Acid.* Citrate ions, usually generated from citric acid or sodium citrate, have been

(36) Washio, I.; Xiong, Y.; Yin, Y.; Xia, Y. *Adv. Mater.* **2006**, *18*, 1745–1749.
(37) Pastoriza-Santos, I.; Liz-Marzán, L. M. *Nano Lett.* **2002**, *2*, 903–905.
(38) Zhang, J.; Liu, H.; Zhan, P.; Wang, Z.; Ming, N. *Adv. Funct. Mater.* **2007**, *17*, 1558–1566.
(39) Germain, V.; Li, J.; Ingert, D.; Wang, Z. L.; Pileni, M. P. *J. Phys. Chem. B* **2003**, *107*, 8717–8720.
(40) Germain, V.; Brioude, A.; Ingert, D.; Pileni, M. P. *J. Chem. Phys.* **2005**, *122*, 124707.
(41) Brioude, A.; Pileni, M. P. *J. Phys. Chem. B* **2005**, *109*, 23371–23377.
(42) Chen, S.; Carroll, D. L. *Nano Lett.* **2002**, *2*, 1003–1007.
(43) Hao, E.; Kelly, K. L.; Hupp, J. T.; Schatz, G. C. *J. Am. Chem. Soc.* **2002**, *124*, 15182–15183.
(44) Henglein, A.; Giersig, M. *J. Phys. Chem. B* **1999**, *103*, 9533–9539.
(45) Pillai, Z. S.; Kamat, P. V. *J. Phys. Chem. B* **2004**, *108*, 945–951.
(46) Enustun, B. V.; Turkevich, J. *J. Am. Chem. Soc.* **1963**, *85*, 3317.
(47) Turkevic, J.; Kim, G. *Science* **1970**, *169*, 873.
(48) Ji, X.; Song, X.; Li, J.; Bai, Y. *J. Am. Chem. Soc.* **2007**, *129*, 13939.
(49) Kamat, P. V.; Flumiani, M.; Hartland, G. *J. Phys. Chem. B* **1998**, *102*, 3123–3128.
(50) Kilin, D. S.; Prezhdo, O. V.; Xia, Y. *Chem. Phys. Lett.* **2008**, *458*, 113–116.
(51) Mpourmpakis, G.; Vlachos, D. G. *Langmuir* **2008**, *24*, 7465–7473.
(52) López-Macipe, A.; Gómez-Morales, J.; Rodŕguez-Clemente, R. *J. Colloid Interface Sci.* **1998**, *200*, 114.
(53) Parkinson, J. A.; Sun, H. Z.; Sadler, P. J. *Chem. Commun.* **1998**, *8*, 881–882.
(54) Jiang, X. C.; Zeng, Q. H.; Yu, A. B. *Nanotechnology* **2006**, *17*, 4929–4935.
(55) Jiang, X. C.; Zeng, Q. H.; Yu, A. B. *Langmuir* **2007**, *23*, 2218–2223.
(56) Zeng, Q. H.; Jiang, X. C.; Yu, A. B.; Lu, G. *Nanotechnology* **2007**, *18*, 035708.
(57) Jiang, X. C.; Yu, A. B. *Langmuir* **2008**, *24*, 4300–4309.

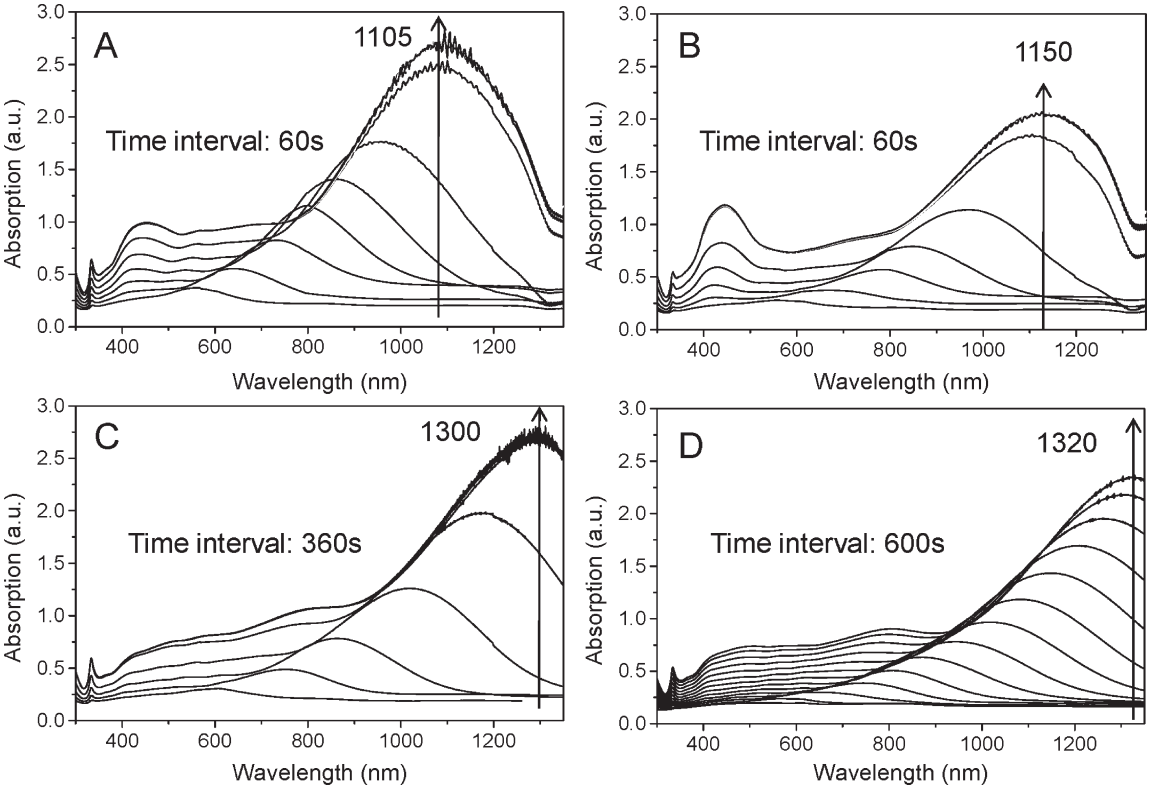

Figure 1. UV−vis spectra showing the formation and growth of silver nanoparticles at different molar ratios of citric acid to silver ions: (A) 3, (B) 6, (C) 12, and (D) 48.

extensively used in the synthesis of silver or gold nanoparticles.[28−57] In order to investigate the role in the synthesis of silver nanoplates, the molar ratio of [cit]/[Ag^+] was adjusted from 3 to 6, 12, 24, and 48 and other parameters were kept constant. The change of the pH is estimated to be $\Delta pH \leq 0.5$ in the solution (pH ~ 5) when the molar ratio of [cit]/[Ag^+] is adjusted in the range of 3−48. UV−vis spectra show the formation and growth of silver nanoparticles that are largely dependent on the molar ratio of citric acid to silver, as shown in Figure 1. At a low ratio of [cit]/[Ag^+] = 3, 6, 12 (Figure 1A−C), the reaction took ~10 min for the strongest plasmon resonance to reach the maximum absorption intensity. When [cit]/[Ag^+] was increased to 24, it took ~50 min to obtain the maximum absorption intensity, while at a high molar ratio of [cit]/[Ag^+] ≥ 48, the reaction became significantly slow and it took ~135 min (Figure 1D). That is, the higher the concentration of citrate ions, the slower the reaction rate under the considered conditions. This is probably caused by the formation of silver citrate complexes if more citrate ions exist in the reaction solution, which can decrease the reducing rate and hence the reaction time to reach the maximum absorption intensity.

This can be further confirmed by the kinetic analysis of the growth process of silver nanoplates. The relationship between the wavelength of the strongest plasmon resonance absorption (λ_{max}) and reaction time (t) was plotted and is shown in Figure 2. As is well-known, the position of the maximum absorption peak, λ_{max}, is strongly dependent on the dimensions of the silver particles.[27−43] λ_{max} is dependent on the growth rate of the silver particles. The value of $d\lambda_{max}/dt$ in this experiment shows the reaction rate, which was calculated to be 0.96, 0.96, 0.79, 0.23, and 0.10, corresponding to [cit]/[Ag^+] of 3, 6, 12, 24, and 48, respectively. That is, the more the citric acid, the slower the growth of silver nanoparticles. In the meantime, the shift in the

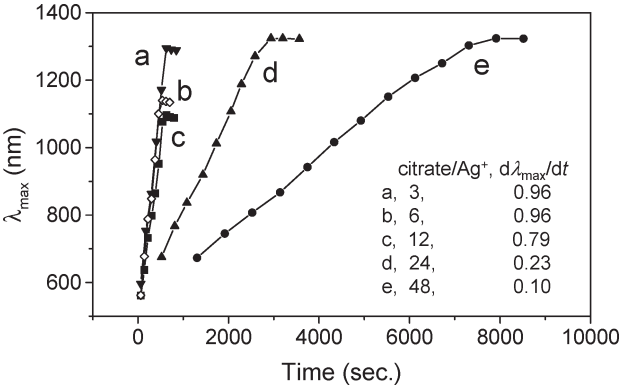

Figure 2. Kinetic analysis showing that the reaction rate decreases from 0.96 to 0.96, 0.79, 0.23, and 0.10 when the molar ratio of citric acid to silver increases from 3 to 6, 12, 24, and 48, respectively.

strongest plasmon resonance absorption to longer wavelengths from 1105 ([cit]/[Ag^+] = 3) to 1150 ([cit]/[Ag^+] = 6), 1300 ([cit]/[Ag^+] = 12), and 1320 nm ([cit]/[Ag^+] = 48) suggests that the particle size or edge length of the triangular silver nanoplates gradually increases, as evidenced by the TEM technique.

TEM images of silver nanoparticles generated at different molar ratios of [cit]/[Ag^+] of 3, 6, 12, and 48 were recorded (see Figure S1 in the Supporting Information, SI). The obtained nanoplates are a majority in the product, along with some nonplatelike particles (e.g., spheres or short rods). The average edge length of the silver nanoplates increases from 100 to 350 nm with an increase in the amount of citric acid. The electron diffraction rings recorded in the SAED patterns in the insets of the two figures show that they are well-crystallized, consistent with the experimental observations in our recent work.[54−57] The nearly spherical particles have an average diameter of 50 nm at

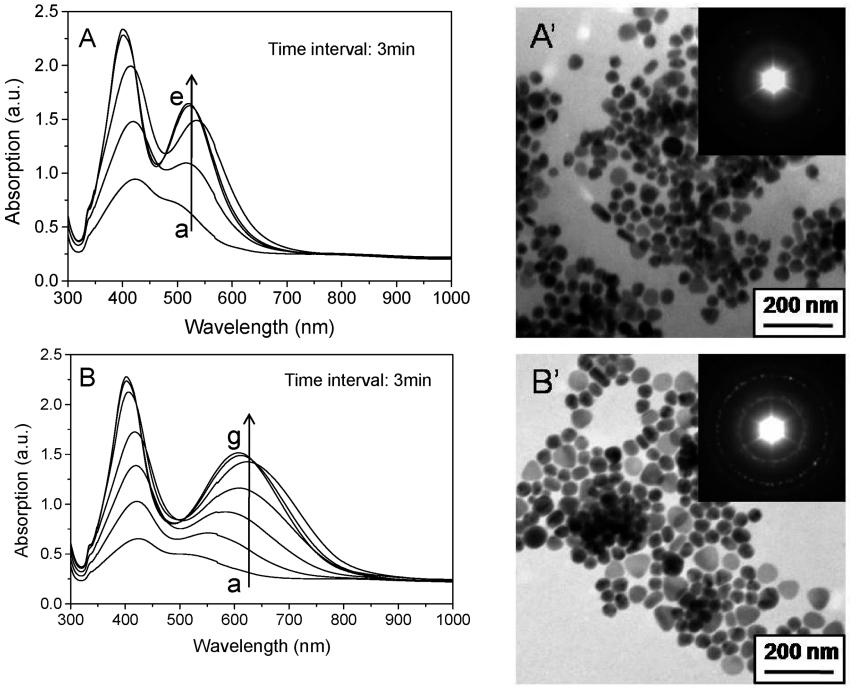

Figure 3. Time-dependent UV−vis spectra of silver nanoparticles on the molar ratio of sodium citrate to silver ions: (A) 6 and (B) 12. Corresponding TEM images (A′ and B′) when the maximum absorption intensity is reached.

lower molar ratios ([cit]/[Ag^+] ≤ 6; Figure S1A,B in the SI). When the ratio of [cit]/[Ag^+] was raised to 12−48, some small nanocrystals (a few nanometers in diameter) coexisted with silver nanoplates (Figure S1C,D in the SI). From the view of reaction kinetics, the lower the molar ratio of [cit]/[Ag^+], the faster the reaction. This is favorable for the nucleation of both spherical and platelike particles, and they can grow bigger simultaneously, while the higher the molar ratio of [cit]/[Ag^+], the slower the reaction, which is more advantageous for the growth of the plates but for spheres due to the kinetic-controlled growth. In addition, we observed that the ratio of small particles (d < 10 nm) rises with an increase in the molar ratio of [cit]/[Ag^+]. At high citrate concentration (relative to silver), most small clusters will be citrate-complexed and would not interact with silver nanoparticles (electrostatic stabilization). Given that small clusters bind the citrate less strongly than nanoplates, at low citrate concentration (relative to silver), a fraction of small silver clusters (positively charged and neutral) in solution are still uncomplexed. The detailed kinetic study on the relationship between the particle dimensions, plasmon resonance absorption position/intensity, and citrate concentration at different temperatures is in progress.

In tracking the particle formation and growth, it is difficult to take all pictures for the intermediates because of the lack of efficient *in-site* observation of liquid samples by the TEM technique. In this work, we used UV−vis spectrometry, a very useful tool, to track the particle growth process under different conditions (e.g., concentration of citric acid, pH, $NaBH_4$, and L-ascorbic acid), along with some representative TEM images (see Figure S2 in the SI). When the molar ratio of [cit]/[Ag^+] was fixed at 48, in the first 20 min, most of the reaction matter is in the form of aggregate, and the triangular particles were observed in the early period of nucleation, even though only a few triangular particles exist (Figure S2A in the SI). It was observed that the reaction matter developed a few well-shaped particles after 45 min, but the particle aggregation still existed (Figure S2B in the SI). So, the reaction from 20 to 45 min for triangular particles is the length of time between nucleation and early crystal development. At the end of the 90-min reaction, more triangular plates formed and became dominant in the product (Figure S2C in the SI). The reaction period between 45 and 90 min is the first major development of the triangular particles. The period from 90 to 135 min is the second major development for triangular particle growth under the reported conditions. At ∼135 min, the strongest absorption peak centered at ∼1320 nm reaches the maximum intensity, and triangular plates were formed with an edge length of ∼200 nm (Figure S2D in the SI), which is bigger than those observed at 45 min (∼50 nm in edge length) and 90 min (∼110 nm in edge length). This means that the triangular plates keep growing within 135 min through the Ostwald ripening process. This can be further confirmed by kinetic analysis. After 135 min, the value of $d\lambda_{max}/dt$ approaches zero and the reaction may enter postdevelopment of the triangular particles. For example, the triangular plates could convert to intermediates between triangles and circle disks and then to circle disks after aging for hundreds of hours.[54−57]

Sodium Citrate. Sodium citrate was also widely used in the synthesis of silver particles. The solution pH changes from 5 to 5.5 when the molar ratios of sodium citrate to silver were adjusted in the range of 1−48. The citric acid or sodium citrate can cause a slight change in the pH of the solution. To investigate the effect of the solution pH on silver particle growth, we have carried out a series of tests. The UV−vis spectra and TEM images reveal the effect of the pH on the formation of silver nanoparticles in aqueous solution (see Figures S3 and S4 in the SI). At a low pH (e.g., 5), the citrate was monoprotonated [$(citrate)^{2-}$] and hydrogen bonds between the free COOH groups of the citrate molecules shielded the nanoparticles and prevent growth (the van der Waals stabilization mechanism); therefore, silver nanoparticles were obtained. Some of them are of triangular shape with an edge length of ∼100 nm (Figure S4A in the SI). Migration of a hydrogen atom within citric acid activates the electrons of the carboxyl oxygen atom and provides additional binding affinity toward the Ag(111) plane. The preferential binding energy of citric acid to Ag(111) promotes crystal growth along the Ag(100)

surface, which benefits the anisotropic growth of nanoparticles. When the pH is lower than 3.5, the mixed solution is kept clear and no precipitates form. This is probably caused by the strong acidic solution, which could dissolve the silver nuclei at the initial stage; thus, no particles form. While at higher pH (>8) the free-in-solution carboxyl group is deprotonated [$(citrate)^{-3}$], no hydrogen bonding occurs between citrate molecules, which can grab silver clusters to the nanoparticle surface, resulting in irregular-shaped particles. It was also observed that the addition of NaOH could result in a quick color change from clear to gray, suggesting the formation of AgOH ($k_{sp} = 2 \times 10^{-8}$) under such high basic conditions. The formation of AgOH could lead to the removal of Ag^+ and also passivation on the silver particle surface to inhibit further redox reaction and particle growth.[58−60] This is also confirmed by the single curve in the UV−vis spectra (Figures S3C,D in the SI) at higher pH values (e.g., 8 and 9.5). Therefore, only a small pH window is suitable for the formation of silver nanoplates at around pH = 5.5; the citrate is monoprotonated [$(citrate)^{2-}$].

Figure 3 shows the UV−vis spectra and the corresponding TEM images of silver particles at different molar ratios of sodium citrate to silver ions (noted as [citrate]/[Ag^+]). When the molar ratio was fixed at 6, the UV−vis spectra of particles were recorded, showing that the reaction took ∼15 min to reach the maximum absorption intensity (Figure 3A). Two strong absorption peaks are observed: one is centered at ∼400 nm and another at ∼530 nm. These two plasmon resonances may have originated from silver particles of different morphologies, as evidenced by the TEM image shown in Figure 3A′. When [citrate]/[Ag^+] was increased to 12, it would take ∼21 min to reach the maximum absorption intensity. Two strong plasmon resonances are centered at around 400 and 600 nm, respectively (Figure 3B). Compared with the sample shown in Figure 3A, the first plasmon resonance band centered at ∼400 nm does not change the absorption position, while the second one shifts to longer wavelengths with time from 530 to 600 nm, suggesting that the size of the generated silver particles increases, as confirmed by the TEM images (Figures 3A′,B′). In addition, it was noted that the last maximum absorption has a slight blue shift in the UV−vis spectra. Two possible reasons can explain such a blue shift: (i) the size of the particles decreases a little because of surface atomic reconstruction with time, and (ii) a small number of the particles transfer their shapes from anisotropic (e.g., triangles) to spherical ones or circular disks because of minimization of the surface energy through surface atomic reconstruction in the final growth stage. TEM images show that the average size of the silver particles increases from 50 to 80 nm, as shown in parts A′ and B′ of Figure 3, respectively. That is, the larger the molar ratio of [citrate]/[Ag^+], the slower the reaction rate and the larger the formed silver particles. This is in agreement with the observations in the growth of silver nanoplates when increasing the concentration of citric acid (Figure S1 in the SI). On the basis of the above experimental observations, one common feature reflected by both citric acid and sodium citrate is the bigger the ratio of citrate to silver ions, the slower the reaction rate and, hence, the bigger the silver particles obtained.

3.2. Role of Citrate Ions. On the basis of the aforementioned experimental observations, citrate ions may show multiple functions in the formation and growth of silver nanoparticles, such as reducing agents, stabilizers, and complexing agents. One or more of the three functions have been reported in different systems in the previous studies, and each of them is still limited to the specific conditions employed.[28−30,44] In our proposed synergistic reduction system, two or three reducing agents (e.g., sodium borohydride, ascorbic acid, and citric acid) are involved, and they could work in a cooperative effort in the formation of silver nanoplates. The citrate ions show some unique features in particle growth and shape control in the present synergistic reduction system. The kinetic analysis further shows that the number of citrate ions can largely influence the reaction rate, particle shape, and size distribution and, hence, the position and intensity of the maximum absorption of surface plasmon resonance. To clearly distinguish the individual functions in such a system is of significant importance.

Reducing Agent. In the proposed approach, it was found that the reducing reaction with sole citric acid takes longer than 1 week to reduce silver ions (the molar ratio of [cit]/[Ag^+] is 3) at room temperature, and the final product shows a wide size distribution. Thus, the citrate ions, as reducing agents, are often used in a boiling solution.[45,46] Silver colloids could be prepared by the well-known Turkevich method in a boiling aqueous system, in which a sodium citrate solution was added drop by drop to the silver nitrate solution when it began to boil.[46] Zeena et al.[45] demonstrated such a reduction reaction when a boiling temperature was used and a prolonged time (>30 min) was important. If the solution was quickly cooled after boiling for 5−15 min, they only obtained partial reduction of silver ions. The citrate ions could serve as weaker reducing agents compared to aqueous electrons, which are produced by radiolysis. Therefore, it is not surprising that the reduction reaction takes over 1 week without the use of light illumination or pulse irradiation at 25 °C, as observed in our system containing surfactant molecules (e.g., AOT). In comparison, it was noted that the solution color could slightly change to light yellow after a few hours without the addition of AOT. This means that the AOT molecules could combine with silver ions to form possible complexes such as Ag_2(AOT), which will largely affect the reducing reaction and hence the formation and growth of silver nanoparticles with different shapes and sizes.

To detect the change of citric acid, a NMR technique was used in this study. The ^{1}H NMR spectra show a peak at $\delta = 2.16$, which could be assigned to acetone (SDBS No. 319HPM-00-026), an oxidation product oxidized by Ag^+ ions, suggesting that the redox reaction occurred in the systems of $AgNO_3$/citric acid and $AgNO_3$/citric acid/AOT (see Figure S5 in the SI) after aging for 1 week at room temperature. Despite the very slow redox rate, this indicates that citric acid has the capability of reducing silver ions in aqueous solution under the reported conditions. When the redox reaction occurs, the citrate oxidation products are carbon oxide and acetone-1,3-dicarboxylate, which can absorb onto silver colloids surface for shape/size control as a capping agent.[51] Under photoirradiation conditions, Wu et al.[61] proposed that unrelaxed, ballistic "hot holes" created in silver plasmon excitation oxidize adsorbed citrate molecules into acetone-1,3-dicarboxylate, which can further decarboxylate to form acetyl acidic acid and acetone by catalysis of silver colloids.[62] However, we need to point out that the peak at $\delta = 2.05$ is unknown at this stage. The systematic study of the reaction system will be performed by NMR in the near future.

On the contrary, sodium borohydride ($NaBH_4$) can serve as a strong reducing agent in the proposed approach. It could lead to a

(58) Caswell, K. K.; Bender, C. M.; Murphy, C. J. *Nano Lett*. **2003**, *3*, 667.
(59) Xue, C.; Mirkin, C. A. *Angew. Chem., Int. Ed*. **2007**, *46*, 2036.
(60) Mpourmpakis, G.; Vlachos, D. G. *Phys. Rev. Lett*. **2009**, *102*, 155505.
(61) Wu, X.; Redmond, P. L.; Liu, H.; Chen, Y.; Steigerwald, M.; Brus, L. *J. Am. Chem. Soc*. **2008**, *130*, 9500–9506.
(62) Munro, C. H.; Smith, W. E.; Garner, M.; Clarkson, J.; White, P. C. *Langmuir* **1995**, *11*, 3712–3720.

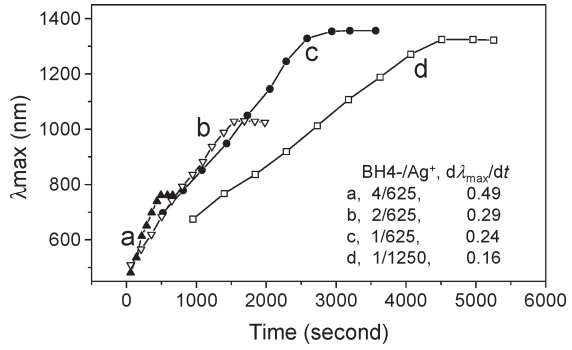

Figure 4. Kinetic analysis showing the reaction rate increases from 0.16 to 0.24, 0.29, and 0.49 when the molar ratio of $NaBH_4$ to silver is raised from 1/1250 to 1/625, 2/625, and 4/625, respectively.

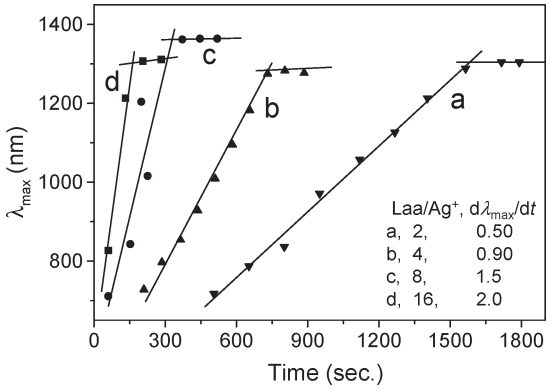

Figure 5. Kinetic analysis showing that the reaction rate increases from 0.5 to 0.9, 1.5, and 2.0 when the molar ratio of L-ascorbic acid to silver is raised from 2 to 4, 8, and 16, respectively.

fast reaction, and the solution color changes quickly even at a low molar ratio of BH_4^- to silver ions (e.g., $[BH_4^-]/[Ag^+] = 1/625$). However, the sole use of $NaBH_4$ can lead to the formation of nearly spherical silver particles (~5 nm) rather than silver nanoplates.[54] If more $NaBH_4$ is added (e.g., 5−10 equiv of Ag^+ ions), the reaction runs very fast and only the final-stage UV−vis spectrum can be recorded. The generated particles are very small in size, of 3−5 nm, and some aggregate together, as described in our recent work.[54] Unfortunately, no triangular particles were obtained at such high ratios of BH_4^- ions. Despite the possible side product (e.g., H_2) for a small ratio of BH_4^- to silver ions, we found that it is the small number of BH_4^- ions that play a key role in the induction of the whole reaction and formation of silver nanoplates. Despite the possible reaction with water, the effect of the side product seems insignificant in our proposed system. This is because the redox reaction of BH_4^- ions with Ag^+ may be faster than that with water because of the high redox potential of Ag^+/Ag^0 (+0.799 V vs NHE) compared with the hydrogen pair ($E^0 = 0$ V).

To track the particle growth clearly, the molar ratio of $NaBH_4$ to silver ions was chosen and adjusted from 1/1250 (A) to 2/625 (B), and 4/625 (C) (see Figure S6 in the SI). The time to reach the maximum absorption intensity is reduced from ~85 min (A) to ~21 min (B) and ~10 min (C), respectively, while the reaction rate increases from $d\lambda_{max}/dt = 0.16$ (curve d) to 0.29 (curve b) and 0.49 (curve a) based on kinetic analysis of the growth process, as shown in Figure 4. In addition, with the increase of the amount of $NaBH_4$ from 1/1250 to 2/625 and 4/625, the position of the maximum absorption peak shifts to short wavelengths from 1370 to 1350 and 1040 nm (Figure S6 in the SI), respectively. The corresponding edge length of the generated silver nanoplates decreases from ~200 (Figure S6A′ in the SI) to ~110 (Figure S6B′ in the SI), and ~70 nm (Figure S6C′ in the SI), respectively. That is, the concentration of BH_4^- ions could heavily influence the formation and growth of silver particles. The small ratio of $BH_4^-]/[Ag^+]$ (e.g., 1/625) may be favorable for the formation of triangular silver particles under the reported conditions.

Compared to citric acid, L-ascorbic acid is slightly stronger in reducing silver ions in the proposed system. Its reducing ability was also tested by altering the molar ratio of L-ascorbic acid to silver ions (noted as $[Laa]/[Ag^+]$) in the synthesis of silver nanoplates. Other experimental parameters (e.g., concentration, molar ratio, and temperature) were kept constant. The time to reach the maximum absorption intensity decreases gradually from ~26 to 13, 8, and 6 min, respectively, confirmed by the UV−vis spectra (see Figure S7 in the SI). Figure 5 shows the kinetic analysis of the formation and growth of silver nanoplates. With an increase in the molar ratio from 2 to 4, 8, and 16, the reaction rate ($d\lambda_{max}/dt$) increases from 0.5 to 0.9, 1.5, and 2.0, respectively. That is, the bigger the molar ratio of $[Laa]/[Ag^+]$, the faster the reducing reaction of the formation of silver nanoparticles under the considered conditions.

Stabilizer. Citrate ions could serve as stabilizers in particle growth and shape control. The stability has been reported in other approaches. For example, Jin et al.[28,29] demonstrated that the citrate ions act as stabilizers in the synthesis of monodispersed silver nanoprisms by visible light or laser illumination. Henglein and Giersig[44] supposed that citrate ions do not act as reducing agents but solely as stabilizers of the colloidal particles formed in the synthesis of colloidal silver sols using ^{60}Co γ irradiation of $AgClO_4$ solutions, by which they prepared silver colloids. Pillai and Kamat[45] demonstrated that citrate ions influence on the particle growth at the early stages by complexing with positively charged Ag_2^+ dimers and slow down the cluster growth contributing to the formation of larger silver nanocrystals of varying shape and size, which also benefits the kinetic-controlled growth of silver particles. Later, theoretical simulation performed by Kilin et al.[50] using ab initio calculations reveals that citric acid is much more likely to bind to the Ag(111) surface than to the Ag(100) surface in particle stabilization. In addition, the citrate oxidation products could be carbon oxide plus acetone-1, 3-dicarboxylate, which can absorb onto silver colloid surfaces for shape/size control as a capping agent.[51] Our ESI mass spectroscopic analysis shows that Ag_2^+(citrate) ($m/z = 408.03$), Ag_2^+(AOT) ($m/z = 637.24$), Ag(citrate)$_2$(AOT) ($m/z = 851.24$), and other clusters can exist in the reaction system, which confirms at least the interaction between silver and citrate ions or AOT molecules (Figure S8 and Table S1 in the SI). They can bind on the surface of the silver clusters and, hence, affect the formation and growth of silver nanoparticles.[54−57]

In our synthesis approach, the citrate ions could also serve as stabilizers in the formation of silver nanoplates, but their stability seems to be weak compared to that of other surfactants tested in our systems, such as AOT, thiols, cetyltrimethylammonium bromide (CTAB), and poly(vinylpyrrolidone) (PVP). It was difficult to generate well-shaped silver nanoplates if no surfactants (e.g., AOT) were added, and the particles are apt to aggregate and precipitate after aging overnight. This is consistent with the observations using the γ-irradiation technique for the preparation of silver colloids. Henglein and Giersig[44] demonstrated that, at a low citrate concentration ($< 10^{-4}$ M), partly agglomerated large particles are formed with many imperfections, while at high citrate concentrations, large lumps of coalesced

silver particles were present because of destabilization by the high ionic strength of the solution.

In this study, the AOT molecules could adsorb on the surface of silver crystals to stabilize the silver particles more effectively and, hence, direct the preferential growth. They prefer to bind on the Ag{111} plane (interaction energy, $E_{int} = -460.1$ kcal·mol^{-1}), which leads to the formation of 2D growth along the Ag{100} (-249.9 kcal·mol^{-1}) or Ag{110} (-323.4 kcal·mol^{-1}) planes.[54] This has been confirmed by experimental observations and numerical simulations (e.g., molecular dynamics method).[54−56] This can be further confirmed in our recent work by the choice of other stabilizers (e.g., CTAB, PVP, and thiols) in shape/size control.[54−57] For instance, the surfactants of PVP and CTAB could result in nearly spherical particles because of the small differences of the interaction energies among three crystalline planes (i.e., 100, 110, and 111), but thiols could lead to platelike particles combining with AOT molecules because of the stronger interaction with the Ag{111} (-959.0 kcal·mol^{-1}) planes than with the Ag{100} (-308.6 kcal·mol^{-1}) and Ag{110} (-361.1 kcal·mol^{-1}) planes under the reported conditions.[56] Nevertheless, it is clear that the citrate ions could serve as stabilizers in the formation of silver nanoplates in the present system.

Complexing Agent. Citrate ions could serve as complex agents in the proposed synthesis process. The experimental observations reveal that the reaction time to reach the maximum absorption intensity was significantly prolonged from ~10 to 135 min when [cit]/[Ag^+] was varied from 3 to 48 (Figures 1 and S1 in the SI). Correspondingly, kinetic analysis shows that the reaction rate ($d\lambda_{max}/dt$) decreases from 0.96 to 0.10. A similar scenario was observed in using sodium citrate (Figure 3). This means that the increase of the citrate ions can significantly lower the reaction rate, which is probably caused by the formation of complexes with silver ions in an aqueous solution. As is well-known, citrate ions in the solution have from one to three carboxylate groups depending on the pH of the solution. They can form strong complexes with metal cations (e.g., Ag^+, Fe^{3+}, Ca^{2+}, Mg^{2+}, and Zn^{2+} ions).[30,45,52,53,63] Two kinds of silver citrate complexes may be formed in the solution: one can be shown as [$Ag_2^+\cdots$citrate],[45] and another one is generally stated as $[Ag_3(C_6H_5O_7)_{n+1}]^{3n-}$, where $n = 1, 2, 3, \ldots$. (Note that $C_6H_5O_7^-$ is the chemical formula of citrate).[63]

For the first, [$Ag_2^+\cdots$citrate] has been studied in the pulse radiation process by Pillai and Kamat,[45] who demonstrated that citrate ions can influence the particle growth at an early stage in the formation of complexing Ag_2^+ dimers. They also evaluated the complexing process by monitoring the transient decay of the absorption peak at 310 nm as the concentration of citrate ions was increased, indicating that the Ag_2^+ ions stabilize as they complex with citrate ions and their conversion to Ag_4^{2+} becomes slower during radiolysis of an aqueous solution. Initially, in the citrate reduction procedure by pulse radiation, few silver seeds are formed. Thus, the seeds formed a strong complex with citrate anions. As the citrate complex slowly grows further by aggregation, it reaches an optimal size, at which stage the strong repelling layer of citrate prevents aggregation. As the smaller particles are oxidized, the Ag^+ ions reabsorb on the larger silver crystallites and undergo reduction at the metal surface.[64,65] Despite not having used radiolysis in our case, the use of reducing agents of both L-ascorbic acid and $NaBH_4$ could reduce Ag^+ ions to Ag^0 atoms and then probably form dimers of Ag_2^+ in aqueous solution at the initial stage, which can be expressed by eqs 1 and 2.

$$Ag^+ + e \rightarrow Ag^0 \quad (1)$$

$$Ag^0 + Ag^+ \leftrightarrow Ag_2^+ \quad (2)$$

Subsequently, the citrate ions may lead to the formation of a silver complex, [$Ag_2^+\cdots$ citrate] (eq 3), which can greatly slow down the formation and growth of silver nanoparticles.

$$Ag_2^+ + \text{citrate}^- \leftrightarrow [Ag_2^+\cdots\text{citrate}^-] \quad (3)$$

This hypothesis can be verified by the ESI mass spectrometry measurements. The intensive peaks at $m/z = 215-216$ and 408.3 show the existence of Ag_2^+ and Ag_2^+(citrate) clusters in the present system (Figure S8 and Table S1 in the SI). The existence of other kinds of silver clusters (e.g., Ag_4^{2+}, Ag_8^{4+}, Ag_3^+, or Ag_3) has been investigated in the past. Henglein[66] has shed some light on the nucleation process by controlling the generation of zerovalent atoms and thus their agglomeration into small clusters in a γ-radiation-based synthesis. Both UV−vis spectroscopic and scanning tunnelling microscopic studies of these clusters suggested that Ag_4^{2+} and Ag_8^{4+} were the most abundant species involved in the nucleation stage.[67] Growth of these clusters into nanocrystals likely occurred through a combination of aggregation and atomic addition. Xia et al.[68] demonstrated that there exists a smaller cluster, Ag_3^+ or Ag_3, in the nucleation stage of a solution-phase synthesis that employed $AgNO_3$ as a precursor to silver nanoparticles. These trimeric clusters can serve as nuclei for the addition of newly formed silver atoms and eventually lead to the formation of triangular nanoplates.

The second silver citrate complex, $[Ag_3(C_6H_5O_7)_{n+1}]^{3n-}$, can be formed by silver ions and citric acid in an aqueous solution demonstrated by Djokić.[63] When the molar ratio of [cit]/[Ag^+] is raised to 48, the value of $[Ag^+]^3\cdot[C_6H_5O_7^{3-}]$ is higher than the solubility of $Ag_3C_6H_5O_7$ ($K_{sp(Ag_3C_6H_5O_7)}$), estimated to be on the order of magnitude $10^{-12}-10^{-11}$). However, no precipitates were observed in the present reaction system because they are expected to be soluble and stable in water, as described in the previous study.[63] Our ESI mass spectrometry analysis could confirm the existence of $[Ag_3(citrate)_2]^{3-}$ clusters in the reaction system (Figure S8 and Table S1 in the SI). Such complexes, $[Ag_3(C_6H_5O_7)_{n+1}]^{3n-}$, still have a tendency to undergo reduction to silver(0) in an aqueous solution, as is seen with reducing agents such as ascorbate or tartrate. Therefore, L-ascorbic acid and $NaBH_4$ could lead to the reduction of silver ions even though such complexes are formed, which can slow the reaction. As discussed above, the existence of silver citrate complexes as either [$Ag_2^+\cdots$citrate] or $[Ag_3(C_6H_5O_7)_{n+1}]^{3n-}$ or both plays a dominant role in slowing the reducing reaction of Ag^+ to Ag^0 and hence the growth of silver nanoparticles. Here we should point out that our proposed synthesis method is a comprehensive reaction and all of the involved components (e.g., AOT, citrate ions, L-ascorbic acid, and $NaBH_4$) could work in a cooperative effort; the number of such complexes is difficult to estimate exactly at this stage.

(63) Djokić, S. *Bioinorg. Chem. Appl.* **2008**, 436458 (7 pages).
(64) Henglein, A.; Meisel, D. *Langmuir* **1998**, *14*, 7392–7396.
(65) Meisel, D. *J. Am. Chem. Soc.* **1979**, *101*, 6133–6135.
(66) Henglein, A. *Chem. Phys. Lett.* **1989**, *154*, 473.
(67) Belloni, J.; Mostafavi, M.; Remita, H.; Marignier, J. L.; Delcourt, M. O. *New J. Chem.* **1998**, *22*, 1239.
(68) Xiong, Y.; Washio, I.; Chen, J.; Sadilek, M.; Xia, Y. *Angew. Chem., Int. Ed.* **2007**, *46*, 4917–4921.

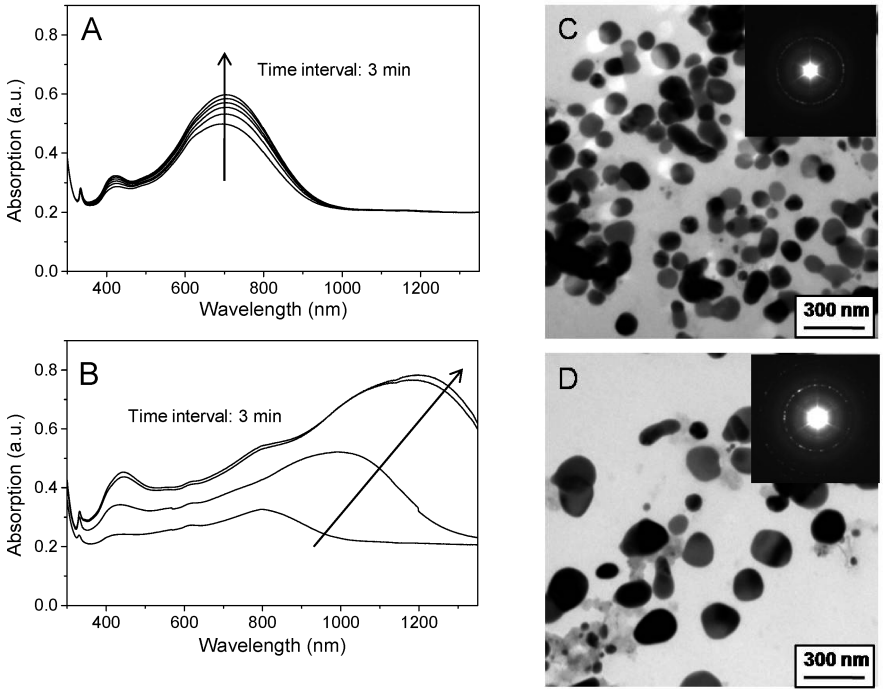

Figure 6. UV−vis spectra (A and B) and the corresponding TEM images (C and D) showing the influence of the molar ratio of $[Fe(CN)_6]^{4-}$ to silver ions on the formation and growth of silver nanoplates.

As a further confirmation, iron hexacyanide ($[Fe(CN)_6]^{4-}$) ions were used to form a complex with silver ions, $Ag_4[Fe(CN)_6]$, which may influence the reducing rate and hence the shape and size of the silver particles because of its strong stability constant ($K_{sp} = 1.55 \times 10^{-39}$).[69] Figure 6 shows the UV−vis spectra (A and B) and the corresponding TEM images (C and D) of silver particles generated by adding appropriate $[Fe(CN)_6]^{4-}$ ions. When the molar ratio of ($[Fe(CN)_6]^{4-}$) ions to silver ions was fixed at 1:4, the synergetic reduction reaction occurred by using both L-ascorbic acid and $NaBH_4$. It took ~10 min to reach the maximum absorption intensity. The UV−vis spectra were recorded and shown in Figure 6A, in which three plasmon resonances emerge and the strongest one is centered at around 700 nm. The corresponding TEM image shows that the particles are of spherical shape with sizes of 50−180 nm (Figure 6C); unfortunately, no triangular silver particles were generated. While the molar ratio of $[Fe(CN)_6]^{4-}$ ions to silver ions was fixed at 1:5, fewer silver ions were used when complexing with $[Fe(CN)_6]^{4-}$ ions, and the reduction reaction reaches the maximum absorption intensity and takes around 12 min (Figure 6B). As a function of time, the strongest plasmon resonance shifts to longer wavelengths from 800 (3 min) to 1000 (6 min), 1220 (9 min), and 1250 nm (12 min). This also means that the particle size gradually increases with time. Figure 6D taken from the 12-min specimen shows that the TEM image particles are almost spherical with a wide size distribution. In addition, parts C and D of Figure 6 show the diffraction rings in the SAED patterns of silver particles, indicating that they are of crystalline structure. On the contrary, the reduction reaction became very slow (taking longer than 4 days) when the molar ratio of $[Fe(CN)_6]^{4-}$ ions to silver ions was raised to 1:1, in which more silver ions may form a complex, $Ag_4[Fe(CN)_6]$, although the exact amount of the complex is difficult to estimate exactly.

In the presence of iron hexacyanide ions, no perfect silver triangular particles were observed, which may be due to the following reasons: (i) the formation of complex $Ag_4[Fe(CN)_6]$ may significantly slow the formation of silver nanoparticles, which could lead to a kinetic but thermal dynamic growth control. This could result in anisotropic growth, and the particles are not well-shaped spheres, as shown in Figure 6C,D; (ii) the $[Fe(CN)_6]^{4-}$ charge state of the dopant has shown to possess amphoteric properties. It can function as a shallow electron trap, or ionized donor center, when free.[70−72] This would affect the electron distribution on the surface of silver crystals and, hence, the morphology and size.

A similar scenario was also reported by Cao et al.,[73] who demonstrated that ethylenediaminetetraacetic acid, as a generally used ligand on monomers, can form complexes with Ag^+ ions, so as to slow the reduction kinetics and subsequently kinetically control the formation and growth of nanoplates. In this study, $[Fe(CN)_6]^{4-}$ is redox-active, but it needs to be oxidized to form $[Fe(CN)_6]^{3-}$ ions. Under the reported conditions, $NaBH_4$, L-ascorbic acid, and citric acid all result in reduction atmospheres, so the oxidation reaction from $[Fe(CN)_6]^{4-}$ to $[Fe(CN)_6]^{3-}$ occurs with difficulty. In addition, the $[Fe(CN)_6]^{4-}$ ions can react with Ag^+ quickly to form a complex of $Ag_4[Fe(CN)_6]$ due to the very small solubility in water ($K_{sp} = 1.55 \times 10^{-39}$). This means that the redox reaction for $[Fe(CN)_6]^{4-}$ is less possible. The formation of such a complex, $Ag_4[Fe(CN)_6]$, may significantly slow the formation of silver nanoparticles, which could lead to a kinetic but thermal dynamic growth control and hence affect the shape and size of silver particles. The use of $[Fe(CN)_6]^{4-}$ ions could provide some useful information to identify the function of citrate ions when complexing with silver ions.

(69) Sillen, L. G.; Martell. A. E. *Stability constants of metal−ion complexes*, 2nd ed.; Special Publication 17; The Chemical Society: London, 1964.

(70) Olm, M. T.; Eachus, R. S. *Radiat. Eff. Defects Solids* **1995**, *135*, 101.
(71) Olm, M. T.; Eachus, R. S.; McDugle, W. G. *Bulg. Chem. Commun.* **1993**, *26*, 350.
(72) Baetzoid, R. C. *J. Phys. Chem. B* **1997**, *101*, 1130–1137.
(73) Cao, Z.; Fu, H.; Kang, L.; Huang, L.; Zhai, T.; Ma, Y.; Yao, J. *J. Mater. Chem.* **2008**, *18*, 2673–2678.

4. Conclusions

We have demonstrated that citrate ions can play multiple roles in the synthesis of silver nanoplates in our developed synergetic reduction process, using sodium borohydride, ascorbic acid, and citrate ions simultaneously. These roles are reflected by the function of citrate ions as reducing agents, stabilizers, and complexing agents. In this connection, a few unique features were observed for the system considered, as summarized below.

I As reducing agents, citrate ions make the reduction reaction take 1 week or longer in the formation of silver particles and lead to a wide size distribution. The kinetic study shows that the reducing ability of citrate ions is weaker than that of L-ascorbic acid and/or sodium borohydride under similar conditions. Only the use of three reducing agents simultaneously could result in the formation of well-controlled silver nanoplates at room temperature. In addition, the use of sodium citrate could not result in the formation of silver nanoplates in the system considered.

II As stabilizers, citrate ions can bind on silver surfaces for shape control, but the ability to stabilize silver particles is weaker than that of other surfactants tested in our approach, such as AOT, CTAB, PVP, and thiols. When no AOT molecules were added in the present system, no well-shaped triangular silver particles were generated, and the obtained particles were apt to aggregate and precipitate after aging overnight.

III As complexing agents, citrate ions can form complexes with silver in the form of either $[Ag_2^+ \cdots$ citrate] or $[Ag_3(C_6H_5O_7)_{n+1}]^{3n-}$ or both, as confirmed by ESI mass spectrometry analysis. These complexes can largely influence the formation and kinetic growth of silver nanoparticles. Kinetic analysis reveals that the concentration of the citrate ions could largely influence the reaction rate ($d\lambda_{max}/dt$). The higher the amount of citric acid, the slower the silver nanoparticles grow. Such a complexing effect can be further confirmed by using $[Fe(CN)_6]^{4-}$ ions to form a silver complex, $Ag_4[Fe(CN)_6]$.

The above-mentioned functions reflected that citrate ions would be useful for the shape-controlled synthesis of silver nanoparticles for desirable optical properties in the visible light and/or near-IR regions (400−2500 nm in wavelength). These can find potential applications in optical sensors, probes, surface-enhanced Raman scattering, plasmonics, and biochemical labeling. Despite some success in this area, it is still challenging to generate monodispersed silver nanoplates with high yield and large scale, particularly for those systems involving citrate ions. The mechanism in particle growth and shape control needs to be further understood, including what kind and how strong the interaction is between citrate and silver ions or silver clusters, what the influence of nuclei formed at the initial stage is on the final morphology of particles, and how to avoid or employ the crystal defects for shape control of nanoparticles.

Acknowledgment. We gratefully acknowledge the financial support of the Australia Research Council (ARC) through the ARC Centres of Excellence for Functional Nanomaterials and the Natural Science Foundation of China (Grant NSF50671019). Nuclear magnetic resonance (^{1}H NMR) spectra were obtained on a Bruker AVANCE III 500.13 MHz spectrometer at the UNSW NMR Facility. Mass spectrometric analysis for this work was carried out at the Bioanalytical Mass Spectrometry Facility, UNSW, and was supported, in part, by infrastructure funding from the New South Wales Government as part of its coinvestment in the National Collaborative Research Infrastructure Strategy. X.C.J. thanks Dr. J. Hook and Dr. D. Thomas for valuable discussion on ^{1}H NMR of citrate and is also thankful for the help of T. Jayasena in ESI measurements at the Analytic Centre at UNSW.

Supporting Information Available: Some experimental results including UV−vis spectra, TEM images of the silver nanoparticles, and NMR and ESI mass spectroscopy. This material is available free of charge via the Internet at http://pubs.acs.org.